

MECHANICAL AND STRUCTURAL RESPONSE OF AISI 4135 STEEL AFTER CONTROLLED COOLING PROCESS

Received – Primljeno: 2015-03-06

Accepted – Prihvaćeno: 2015-09-20

Original Scientific Paper – Izvorni znanstveni rad

AISI 4135 steel is a commonly used material for high strength applications such as shafts, forgings and high pressure steel cylinders. The mentioned steel is used in a variety of microalloying by Nb, Ti, V, N, respectively of those elements combinations. In this presented paper, three different microalloyed (by N and V) heats of mentioned steel were studied. Three heat treatment modes were applied. The first mode was based on heating at 700 °C, subsequent quenching and tempering at 470 °C. In the second and the third mode the material was heated at 890 °C and subsequently different controlled cooling process followed in both modes. Microstructural and microfractographic analyses compared with found mechanical properties were part of the solution.

Key words: AISI 4135, heat treatment, control rolling, microstructure, mechanical properties

INTRODUCTION

The AISI 4135 steel type represents a good balance among different properties as strength, toughness, fatigue and corrosion resistance under extreme working conditions and therefore it is used for a variety of industrial and constructional applications, such as, forgings, rolled plates, cranes, wind turbines, mining equipment and also for the production of high pressure steel cylinders (HPSC) and vessels, including compressed natural gas (CNG) transportation and storages etc. [1-4]. Variations of microalloying by Nb, V, Ti, B and N are often used in the AISI 4135 [5, 6]. Steel purity, deformation temperatures, strain rate, chosen heat treatment (HT) and cooling processes (CP) influence the final microstructure and mechanical properties. Nürnberger [2, 3] confirmed the important influence of the cooling rate and strain level on final microstructure, however without accelerated cooling process (ACC) consideration. In [7] authors showed the low cycle lifetime response of 42CrMo4 steel after normalization and after tempering related to the change of modulus of elasticity. Chen [8] detected in steel AISI 4135 quenching cracks caused by uneven surface cooling. Moli-Sanches [9] ascribed higher hydrogen mobility in the AISI 4135 treated at 680 °C than at 540 °C to higher dislocation density and hydrogen trapping.

Nowadays, development of the similar steel 42CrMo4 to AISI 4135 is targeted on maximum strength simultaneously with high toughness and favorable corrosion resistance in a sour environment [4]. This is also the aim of the presented paper.

EXPERIMENTAL PROCEDURE

Samples of 3 heats (AISI 4135) manufactured under the same conditions (Table 1), after hot reserved extrusion from billet and reversed hot rolling (10,2 mm in thickness) including ACC were used.

Table 1 **Average chemical composition of used heats / wt. %**

| C | Mn | Si | Cr | Mo |
|------|-------|-------|--------|------|
| 0,36 | 0,84 | 0,27 | 1,13 | 0,21 |
| P | S | V | N | - |
| 0,12 | 0,004 | 0,073 | 0,0113 | |

Three heat treatment modes were realized. The HT1 was based on the heating at 700 °C, fast cooling in quenching bath (QB) and tempering at 470 °C. The HT2 consisted of a controlled cooling process (CCP) based on the heating to the austenitic zone (γ -zone) with subsequent fast air cooling to the intercritical zone (IZ). Afterwards, fast cooling in QB to the temperature T just above the martensite start (M_s) followed with air cooling to 40 °C under the M_s and cooling (QB) to the room temperature with tempering at 470 °C / air. Further, the heating to γ -zone followed-up air cooling to the IZ with fast cooling (QB) to 200 °C above the M_s and air cooling to 90 °C above the M_s followed by QB cooling to the room T with tempering at 470 °C / air represented the HT3 mode. Testing of mechanical properties was an integral part of the solution. The yield stress and tensile strength ($R_{p0,2}$, R_m), elongation (A), Brinell's hardness (HB) and notch toughness (KCV) parameters were established. Testing of $R_{p0,2}$, R_m and A was realized by use of the Zwick/Roell Z 250 machine (EN ISO 6892-1). The HB was measured using the M4U750 hardness testing machine (EN ISO 6506-1) and KCV was tested by

P. Kučera, Vitkovice Cylinders Inc., Czech Republic
E. Mazancová, VŠB - Technical University of Ostrava, Faculty of Metallurgy and Materials Engineering, Czech Republic

use of the RKP 450 Charpy Impact Testing Machine (ISO 148-1) at $-50\text{ }^{\circ}\text{C}$. Metallographic evaluation was carried out using a light microscope Neophot 21 (purity - ČSN ISO 4967), microstructure analysis, the grain size ($G\gamma$) - ASTM E 112. For micro-fractography transverse KCV samples were used (SEM JEOL JSM-6490).

Table 2 Resulting mechanical properties and grain size ($G\gamma$) of three heats after three different modes of heat treatment

| HTM | HT1 | HT2 | HT3 |
|---|------|-------|-------|
| $R_{p0.2}$ / MPa | 676 | 1 120 | 1 272 |
| R_m / MPa | 824 | 1 257 | 1 397 |
| A / % | 17,6 | 12,5 | 9,8 |
| $KCV_{trans.}$ / $\text{J}\times\text{cm}^{-2}$ | 22 | 34 | 23 |
| $KCV_{long.}$ / $\text{J}\times\text{cm}^{-2}$ | 19 | 35 | 22 |
| HB (2,5 / 187,5) / - | 248 | 402 | 424 |
| $G\gamma$ / grade | 10 | 11 | 8 |

RESULTS AND DISCUSSION

The lowest levels of strength and KCV properties were found in the case of HT1. In both testing directions, KCV values showed an insignificant difference of $3\text{ J}\times\text{cm}^{-2}$. After HT2 application tensile properties were lying between the HT1 and HT3 values, however balanced KCV values in both testing directions were significantly higher than those in cases of HT1 and HT3. The resulting A and HB values fully correspond with the upward trend of tensile properties as can be seen in Table 2 including the $G\gamma$. The non-metallic inclusions evaluation of all three heats revealed a considerably high purity level of all investigated heats. Fine sulphides were revealed once (HT3) of the 1,1 grade. Aluminates were not detected, silicates were in the range from 0 - 0,5 and fine oxides from 0,1 - 0,8. The most favorable and balanced values of tensile properties and KCV in both testing could be ascribed to the HT2 with the finest $G\gamma$.

Microstructure was evaluated from the areas close to the inner surface of the semi-product of HPSC. The reason for this choice of place is the most commonly used HT of cylinders in closed state. Namely, there is no access of the quenching medium to the inner surface of cylinders. This causes heating of the inner and slightly under the inner surface area of the cylinder by trapped gases for a longer time than the outer surface, where the cooling rate is much higher due to direct contact with the quenching medium. This results in more noticeable segregation banding in the inner under surface area due to longer times for possible segregation processes. Microstructure after the HT1 predominantly revealed low bainite (LB) partially mixed with ferrite (F), low portion of acicular ferrite (AF) and pearlite (P) - see Figures 1a,1b. This was also the reason for the 34 % lower R_m of the HT1 in comparison with the HT2. Microstructure after the TH1 is similar to the microstructure after the slow air cooling after the hot forming temperatures

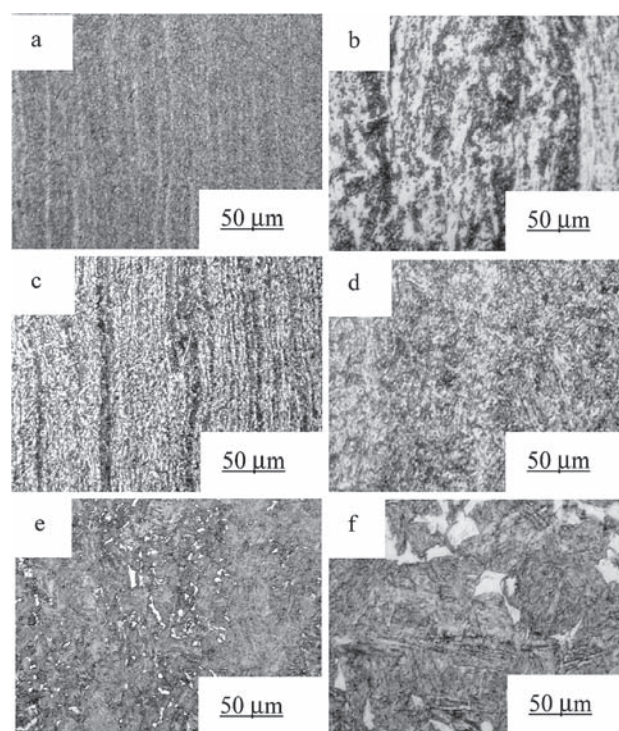


Figure 1 Micrographs (Nital) of a) HT1- general view, b) HT1- detail, c) HT2 - general view, d) HT2 - detail, e) HT3 - general view, f) HT3 - detail

of reverse rolling which allowed significant segregation of elements such as Cr, Mo, and C to the segregation bands, which are moderately thick and of continuous character as shown in Figures 1a – 1d.

The heating at $700\text{ }^{\circ}\text{C}$ was approx. $25\text{ }^{\circ}\text{C}$ under the A_{c1} due to deficient heating temperature and the austenitization process was not achieved. Resulting coarse microstructure (grade 10) contained numerous carbide particles, which precipitated during the tempering process. Significantly banded microstructure, which originated during the process of forming and subsequent cooling, was not reduced due to low heating temperature. Resulting tensile properties fully correspond with the microstructure and the differences of KCV values (Table 2), in which testing KCV values (Table 2), in which testing directions are consistent with the segregation banding in the microstructure. Figures 1c and 1d represent microstructure of finer morphology obtained after the HT2 application with significantly reduced segregation bands (thinner and discontinuous).

This corresponds with the highly balanced KCV results in both testing directions as well as highly balanced strength and KCV parameters (Table 2). Microstructure consists of fine tempered martensite (α'), AF and LB in small portion. The phase of AF was obtained by cooling on the air from the fully γ -zone to the IZ, which is able to suppress harmful segregation banding. Presented oxisulfidic inclusions supported AF nucleation and Mo in steel modified its shape. Subsequent fast cooling in the QB to the T just above the M_s ensured restriction of the segregation processes to the minimum according to the resulting reduced banded microstructure.

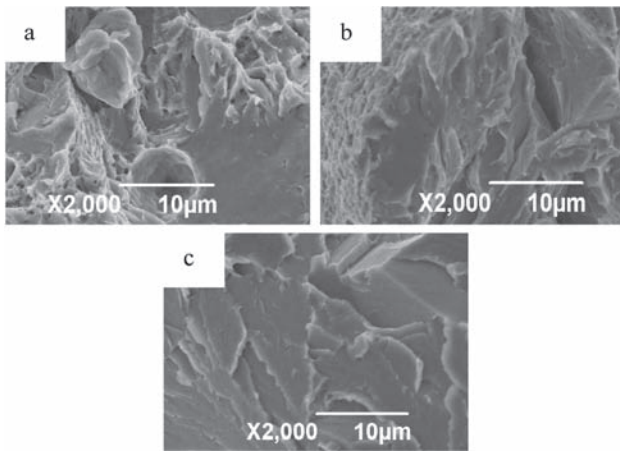


Figure 2 Fracture surface of CVN specimen after a) HT1, b) HT2, c) HT3

ture. Cooling in air to the $T = 40\text{ }^{\circ}\text{C}$ resulted in partial LB and by subsequent quenching in QB, the α' microstructure was obtained.

The microstructure after the HT3 application (Figures 1e, 1f) is formed by tempered α' , AF and polygonal F. Both after the HT2 and the HT3 application, the AF phase was obtained due to the cooling from fully γ -zone to the IZ and segregation banding was considerably eliminated, however cooling in air from $200\text{ }^{\circ}\text{C}$ to $90\text{ }^{\circ}\text{C}$ above the M_s before cooling in QB, caused undesirable extended polygonal F formation which disrupts the microstructure homogeneity and from the point of view of mechanical properties e.g. sulfide stress cracking resistance. This phenomenon appeared due to the long-lasting cooling in air from $200\text{ }^{\circ}\text{C}$ to $90\text{ }^{\circ}\text{C}$ with the contribution of hot trapped gases inside of the heat treated cylinder which were continuously heating the inner and under inner surface area of the material. Restriction of noticeable segregation banding was directly reflected in balanced *KCV* values in both testing directions (see Table 2).

The (α') transformation occurred as a result of fast cooling in the QB from the temperature of $90\text{ }^{\circ}\text{C}$ above M_s to the room temperature. By subsequent tempering, primarily tempered (α') phase and the precipitation of carbide particles in (α') and LB was formed as was observed after the HT2 application. The achieved higher $R_{p0.2}$ and R_m levels resulted from higher quenching temperature used to realize the quenching as compared with the HT2 mode. Observed coarser $G\gamma$ might probably cause decrease of the *KCV* and elongation values together with higher level of tensile properties. As Figure 2 shows, fractured *KCV* specimens showed coarser trans-crystalline cleavage character (HT1, HT3) and/or quasi-cleavage facets with ductile ridges (HT2). Their occurrence was sporadic and found ridges were very thin. The reason for the disproportional values of *KCV* in transverse and longitudinal testing direction (Table 2) is continual thicker banding. This observed fracture surface corresponds with the achieved mixed microstructure of LB, P and AF and also confirms the lowest achieved *KCV* values (Table 2) correlating with [6].

Fracture surface of specimens after the application of HT2 revealed similar character of fracture surfaces like in the of HT1, however cleavage and/or quasi-cleavage facets were significantly finer and more even, corresponding to the found grain size (Table 2), partially decorated with thin ductile ridges and also thicker and longer ductile ridges were observed (Figure 2c). This was the cause of increased *KCV* values. Finer microstructure and partial elimination of unfavorable segregation banding of the HT2 microstructure unlike the HT1, contributed to balanced tensile properties and *KCV* levels. Figure 2 demonstrates the fracture surface of the *KCV* specimen after the application of HT3. In this case, the fracture surface showed rather trans-crystalline cleavage character with creeks detected in some facets. In given case, the facets were the coarsest. Ductile ridges were observed sporadically and were thin and short. This morphology fully corresponds with the lowest grain size of used HT2 compared to the other two used treatments with finer grain size. Fracture surface character also corresponds with the highest tensile properties showing the lowest elongation value.

CONCLUSIONS

The paper summarizes the results of mechanical properties, metallographic and fractographic observations of three different heat treatment modes of the AISI 4135. The best achieved results of achieved mechanical properties from the point of view of tensile properties vs. balanced and high *KCV* in two testing directions were seen in case of HT2, where the segregation banding in microstructure was significantly restricted in comparison with the HT1 and HT3 modes. Microstructure obtained by the HT2 mode revealed slight discontinuous banding and its elimination would be possible by increasing the cooling rate from the γ -zone to IZ. The subsequent time and tempering temperature should be increased in order to moderately increase the values of *A* and *KCV* at the cost of a moderate R_m decrease to approx. $1\ 200\text{ MPa}$. This experimental procedure proved that the most influencing factor of high tensile properties and as high values of *KCV* as possible is the grain size as it was reported in [6].

Acknowledgements

This paper was created in company Vítkovice Cylinders Inc. and at the FMMI in the Project No. LO1203 “Regional Materials Science and Technological Centre – Feasibility Program” funded by Ministry of Education, Youth and Sports of the Czech Republic.

REFERENCES

- [1] F. Dikmen, M. Bayraktar, R. Guclu, Railway Axle Analyses: Fatigue Damage and Life Analysis of Rail Vehicle Axle, *Strojniški vestnik, J. Mech. Eng.* 58 (2012) 9, 545-552.

- [2] F. Nürnbergger, O. Grydin, M. Schaper, F.W. Bach, B. Koczurkiewicz, A. Milenin, Microstructure transformations in tempering steels during continuous cooling from hot forging temperatures, *Steel Res. Int.* 81 (2010), 224-232.
- [3] F. Nürnbergger, O. Grydin, Yu Z., M. Schaper, Microstructural behaviour of tempering steels during precision forging and quenching from hot-forming temperatures, *Metal. Mining Industry* 3 (2011), 79-85.
- [4] P. Kučera, E. Mazancová, Mechanical and microstructural parameters of 34CrMo4 steel after simulated accelerated cooling process under the Ar3 temperature, *Mat. Eng.* 21 (2014), 61-67.
- [5] L. Rancel, M. Gomez, S. F. Medina, P. Valles, Analysis of V(C, N) nanoparticles in medium carbon bainitic microalloyed steel and their influence on strengthening. *Int. J. Mat. Res.* 104 (2013) 6, 527-534.
- [6] C. I. Garcia, M.J. Hua, A. J. Deardo, W. Gao, R.J. Glodowski, The Transformation and Strengthening Behavior of V-N Steel During Hot Strip Mill Simulation, *Iron and Steel Tech.* 10 (2007) 4, 114-122.
- [7] R. Kunc, I. Prebil, Low-cycle fatigue properties of steel 42CrMo4, *Mat. Sci. Eng. A345* (2003), 278 - 285.
- [8] R. Chen, A. Wu, J. Zhao, Y. Chen, Analysis of surface cracks on gas cylinder of 34CrMo4 steel, *Ph. Exam. Testing* 31 (2013) 2, 53-55.
- [9] L. Moli-Sanchez, L. Martin, F. Leunis, J. Wery, Hydrogen transport in 34CrMo4 Martensitic Steel: Influence of Microstructural Defects on H Diffusion, *Defect and Diffusion Forum* 323-325 (2012), 485-490.
- [10] M. Gouné, J. Bouaziz, M. Pipard, P. Murgis, Etude de L'effect de la deformation sur la formation de l'austénite. *Rv. Métallurgie-CIT* 103 (10) (2006), 466-471.
- Note:** The responsible translator for English language is Radek Musil, Brno, Czech Republic